Long-Line Effect and Pulsed Magnetrons*

W. L. PRITCHARD†

Summary—A simplified theory of long-line effect is developed leading to expressions for maximum tolerable line length and vswr. The theory is verified experimentally and photographic evidence of the deleterious effect of long-line behavior is presented. The prevention of long-line effect by various methods, including decoupling the magnetron, attenuation, phase shifter, and ferrite isolators, is discussed.

I. Introduction

"LONG-LINE Effect" can be defined as the group of phenomena happening when an oscillator is coupled to a long, mismatched transmission line. Its theory is a special case of the more general theory of oscillator operation with reactive loading. It is a serious problem in communications and radar systems at microwave frequencies because most of the available transmitting oscillators must be coupled directly to the antenna system (power amplifiers are still not generally available), and long lengths of transmission line are frequently needed in the installation. Its deleterious effects are erratic AFC operation (in systems using AFC), effective loss in receiver sensitivity and serious distortion in fm systems among others.

The purpose of this paper is to present an elementary theory of the effect, experimental confirmation, and some remedial technique. Pulsed magnetron oscillators will be considered primarily, but most of the theory is general enough to be applied to any oscillator.

II. Simplified Theory

1. *Assumptions and the Magnetron Equivalent Circuit*

We assume here that the magnetron is representable by a shunt resonant circuit and that the resonant frequency is that at which the net susceptance of the magnetron and load is zero. It is possible to develop a more refined theory which considers the effects of magnetron and load conductance, but it is complex and adds very little to the understanding of the problem or its solutions.

Fig. 1 represents the magnetron coupled to a long transmission line by the simple equivalent circuit. We assume a resistive mismatch producing a vswr of ρ at the end of a line of electrical length, θ. If B is the input susceptance of the transmission line, then at the angular frequency of oscillation ω we have

$$B_m + B/n^2 = 0. \tag{1}$$

Since the magnetron has been represented as a shunt resonant circuit, its susceptance is given by

$$B_m = \omega_0 C(\omega/\omega_0 - \omega_0/\omega) \cong 2(\omega - \omega_0)C, \tag{2}$$

where ω_0 is the natural resonant angular frequency of the magnetron. Substituting (2) in (1) yields

$$\omega - \omega_0 = - B/2n^2C. \tag{3}$$

From the standard theory of cavities[1] represented as resonant circuits, we have the relation

$$\omega_0 C = Q_E/n^2. \tag{4}$$

Q_E is defined as the "external Q" of the circuit when the transmission line is terminated in a matched load ($R_0 = 1$). It is the Q resulting from external losses only while Q_0, the "unloaded Q," is defined as the Q resulting from internal losses in the conductance, G, only. Eq. (3) can now be written as

$$\omega - \omega_0 = - B\omega_0/2Q_E. \tag{5}$$

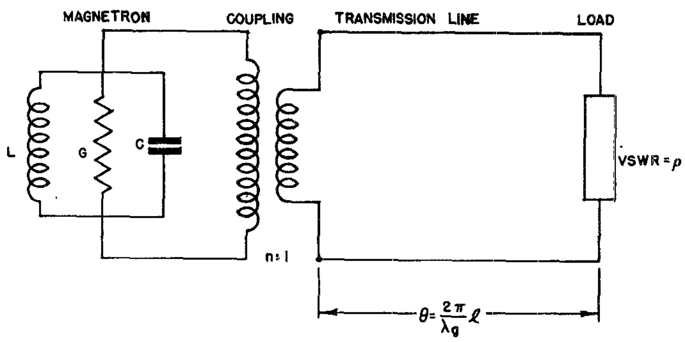

Fig. 1—Equivalent circuit of magnetron coupled to a long mismatched line.

2. *Pulling Figure*

We now define pulling figure, P, as the total excursion of the frequency, f, when the standing wave ratio on the line is equal to 1.5 and is varied through all possible phases. Under these conditions, B, which is the input susceptance of the line, will vary and its total change can be calculated, from the formula for the input admittance of a transmission line, as equal to $\pm .417$ enabling us to eliminate Q_E from (5) by considering f_1 and f_2 as the extreme changes in frequency as B is varied. We can write

$$f_1 = f_0 - .417\, f_0/2Q_E,$$
$$f_2 = f_0 + .417\, f_0/2Q_E.$$

Then

$$P = f_2 - f_1 = .417\, f_0/Q_E, \tag{6}$$

and from (5)

$$\omega_0 = \omega + B\pi P/.417. \tag{7}$$

* This paper was originally presented at the Electron Devices Symposium of the IRE in 1951.

† Raytheon Manufacturing Co., Microwave and Transmitter Branch, Wayland, Mass.

[1] Montgomery, Dickey, Purcell, "Principles of Microwave Circuits," Rad. Lab. Ser., vol. 8, McGraw-Hill Book Company, Inc., New York, N. Y. 1948, pp. 207–239.

Eq. (7), when combined with the expression for B as a function of ω to be derived from conventional line theory, is basic to the whole problem of long-line effect. We would like to relate further the pulling figure of the magnetron to its circuit efficiency. This efficiency, η_c, is defined as the ratio of the power delivered to an external load to the total power available in the resonant circuit. It can be shown that it is related to the unloaded and external Q's of the magnetron by the relation

$$\eta_c = \frac{1}{1 + Q_E/Q_0} = \frac{1}{1 + 1/\beta}, \tag{8}$$

where $\beta = Q_0/Q_E$.

Combining (6) and (8) yields

$$\eta_c = \frac{1}{1 + .417 f_0/PQ_0} = \frac{\beta}{1 + \beta} \cdot \tag{9}$$

$$P = .417 f_0\beta/Q_0.$$

Fig. 2 is a curve of η_c vs β. Since pulling figure is linearly related to β, the coupling factor, Fig. 2 also represents efficiency as a function of pulling figure. It is important to note that at high efficiencies a small change in efficiency produces a very large change in P. This will be elaborated when methods of overcoming the long-line effect are discussed.

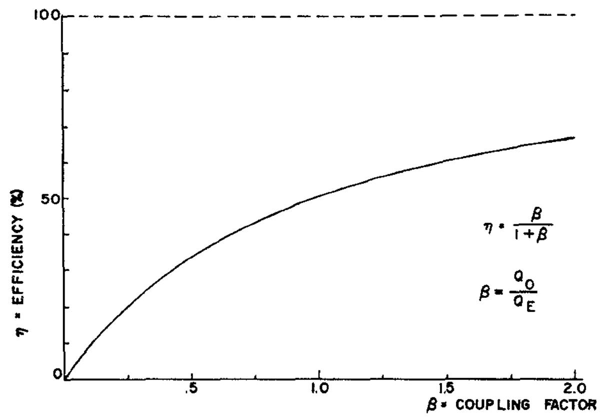

Fig. 2—Efficiency vs coupling factor.

3. *The Susceptance of a Mismatched Transmission Line*

The input admittance of a lossless line is given by

$$Y = \frac{Y_l + j \tan\theta}{1 + jY_l \tan\theta} \cdot \tag{10}$$

Also necessary for the derivation of B are the following standard relations:

$$\Gamma = \frac{1 - Y_l}{1 + Y_l}, \quad \Gamma = |\Gamma| \epsilon^{j\phi}, \quad |\Gamma| = \frac{\rho - 1}{\rho + 1} \cdot \tag{11}$$

Using the relations (11) and separating the imaginary part of (10), we can write, after routine manipulating,

$$B = \frac{-\sin\psi}{\dfrac{\rho^2 + 1}{\rho^2 - 1} + \cos\psi}, \tag{12}$$

where

$$\psi = \phi - 2\theta.$$

Eq. (12) is important. It is the necessary relation between the input susceptance of a transmission line and its length and standing wave ratio and, in combination with (7), will enable us to derive the critical conditions for long-line instability. It is plotted in Fig. 3 for various values of ρ.

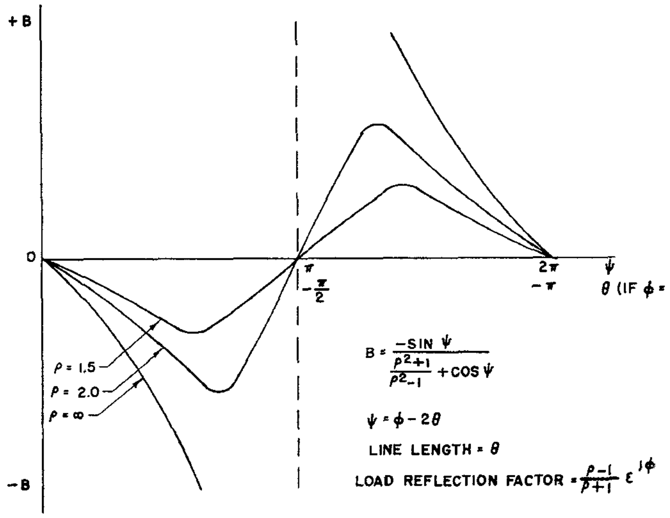

Fig. 3—Line susceptance vs line length.

4. *Magnetron Instability and "Skip Length"*

By substituting the value of B just determined in (7), we have

$$\omega_0 = \omega - \frac{(\pi P/.417) \sin\psi}{\dfrac{\rho^2 + 1}{\rho^2 - 1} + \cos\psi}, \tag{13}$$

where

$$\psi = \phi - 2\theta = \phi - (2\omega/c)(\lambda/\lambda_g)l. \tag{14}$$

The second term of the right side of (13) is a function of ω by virtue of the expression (14) relating ψ to the electrical length of the line. The factor λ/λ_g will be unity on a coaxial line, but for a waveguide will be of the order of magnitude of $\sqrt{2}/2$. Strictly speaking, it is also a function of frequency, since a waveguide is dispersive, but for this discussion it will be assumed constant. Eq. (13) can be plotted vs ω and is shown in Fig. 4. Note that $\omega_0 = \omega$ periodically and this period can be determined by differentiation of (14). $\Delta\omega$, the change in ω between alternate points where $\omega_0 = \omega$ is then found to be

$$\Delta\omega = \frac{\pi}{l} \frac{\lambda}{\lambda_g} c. \tag{15}$$

This equation is extremely important in considering curative measures for instability and will be discussed further. We note here that in a waveguide the period $\Delta\omega$ approaches zero as we come nearer the cutoff frequency and λ_g approaches infinity.

Fig. 4 is plotted for two different values of standing wave ratio. Note that for the higher value of ρ there is the possibility of magnetron oscillation at two frequencies in certain regions of ω_0. These are the regions of instability and are controlled by the phase angle ϕ of the load. If the spectrum of the transmitter signal is narrower than the frequency spread between unstable points, then this phase can be adjusted so as to maintain stable operation. However, this quasi-stable operating condition may not be ideal since the nonlinearity of the curve can cause distortion and alteration of the spectrum width even if there are no actual "jumps" in frequency.

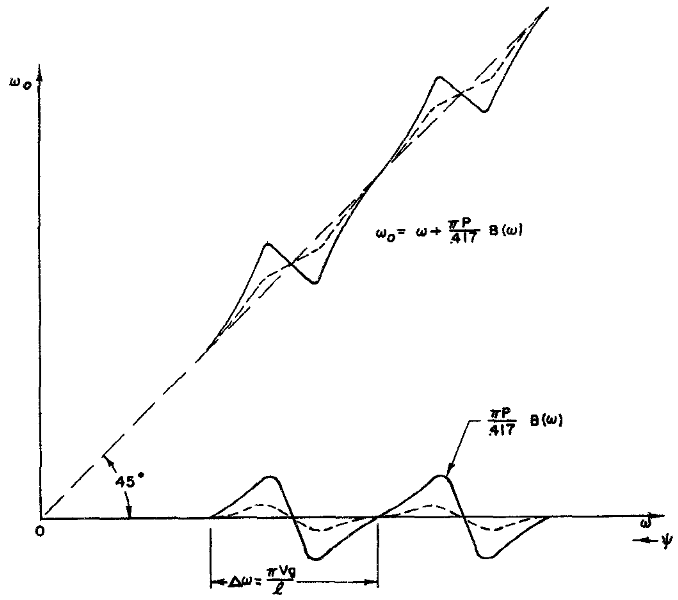

Fig. 4—Magnetron tuning curve.

For completely stable operation, regardless of the phase angle of the load, it is necessary that the curve of ω vs ω_0 be always single-valued. This critical condition is determined by setting the slope $d\omega_0/d\omega$ equal to zero at the points where $\omega_0 = \omega$.

$$\frac{d\omega_0}{d\omega} = 1 + \frac{\pi P}{.417}\left[\frac{1 + \frac{\rho^2+1}{\rho^2-1}\cos\psi}{\left(\frac{\rho^2+1}{\rho^2-1} + \cos\psi\right)^2}\right]\left[\frac{4\pi}{c}\frac{\lambda_g}{\lambda} l\right]\left[\frac{1}{2\pi}\right],$$

letting $\psi = \pi, 3\pi \cdots$ and $d\omega_0/d\omega = 0$, we solve for l to get

$$l_c = \frac{\frac{.417}{\pi P}\frac{\lambda}{\lambda_g} c}{\rho^2 - 1}. \tag{16}$$

l_c is the "skip length" and is the longest length of line for which completely stable operation is possible regardless of load phase angle. Note its dependence on vswr, pulling figure, and proximity to cutoff of the transmission line. Eq. (16) can be rewritten as

$$\frac{l_c}{\lambda_g} = \frac{k/\lambda_g}{\rho^2 - 1}, \tag{17}$$

where

$$k/\lambda_g = \frac{.417}{\pi}\frac{f}{P}\left(\frac{\lambda}{\lambda_g}\right)^2.$$

Eq. (17) is plotted in Fig. 5 for representative values of the variable and parameters. It is important to note that the skip length for a particular vswr is longer at lower frequencies only because the pulling figure of lower frequency oscillators is generally lower and *not* because of the longer wavelength directly.

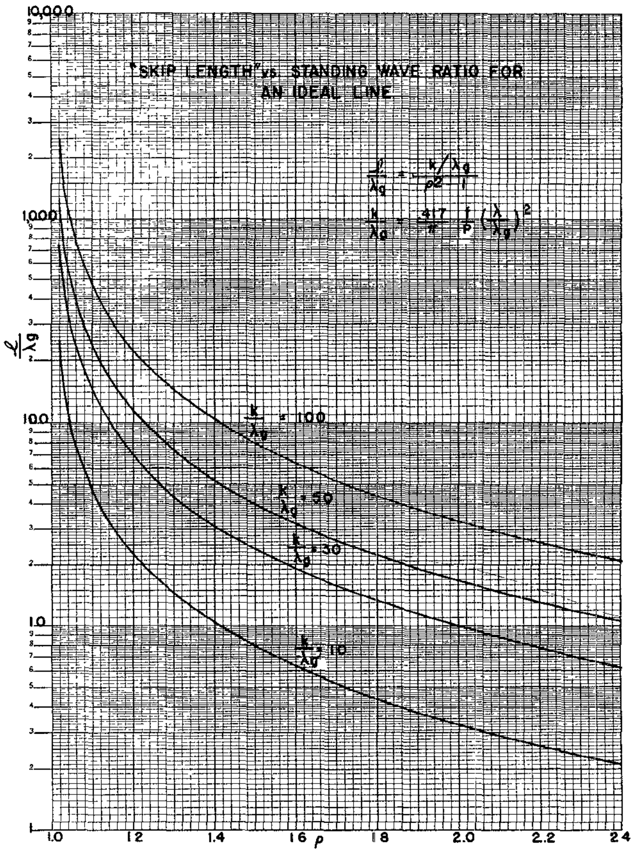

Fig. 5—"Skip length" vs standing wave ratio for an ideal line.

5. *Effect of Line Losses*

The preceding theory has been developed under the assumption that the line is lossless. The effect of loss is to reduce the vswr at the input of the line and hence increase the skip length. The problem can be handled theoretically by assuming that a lossy line is replaceable by a lumped attenuator and a lossless line. Let ρ_l and Γ_l represent the vswr and reflection coefficient of the load and ρ_0 and Γ_0 represent the vswr and reflection coefficient at the input end. They will be different from ρ_l and Γ_l because of the line attenuation α per unit length. We have the following relations from transmission line theory. (A is the total attenuation of a line of length l).

$$\rho_l = \frac{1+\Gamma_l}{1-\Gamma_l} \quad \rho_0 = \frac{1+\Gamma_0}{1-\Gamma_0} \quad \Gamma_0 = \Gamma_l/A^2 \quad A = \epsilon^{\alpha l}. \tag{18}$$

Using the relations (18), we can write, after a little manipulating,

$$\rho_0^2 - 1 = \frac{4\Gamma_l}{(\epsilon^{\alpha l} - \Gamma_l \epsilon^{-\alpha l})^2} \tag{19}$$

or, in terms of hyperbolic functions,

$$\rho_0^2 - 1 = \frac{\rho_l^2 - 1}{(\cosh \alpha l + \rho_l \sinh \alpha l)^2} \cdot \tag{20}$$

The value of $(\rho_0^2 - 1)$ is determined from (17) for the skip length, l_c, and substituted in (20). The result is a quadratic equation for ρ_l which can be solved and the solution written as

$$\rho_l = \frac{\sqrt{\dfrac{k/\lambda_g}{l_c/\lambda_g} + 1} + \dfrac{k/\lambda_g}{2l_c/\lambda_g} \sinh\left[(2\alpha\lambda_g)\dfrac{l_c}{\lambda_g}\right]}{1 - \dfrac{k/\lambda_g}{l_c/\lambda_g} \sinh^2\left[(\alpha\lambda_g)\dfrac{l_c}{\lambda_g}\right]}, \tag{21}$$

where k/λ_g has the same meaning as before. Eq. (21) is plotted in Fig. 6 for representative values of the parameters. Note that for any lossy line, no matter how low the losses, there is ultimately a length for which an infinite vswr can be tolerated. This length can be determined by setting the denominator equal to zero in (21) and solving for l_c. It is usually not of practical significance however, since the loss may be prohibitively high.

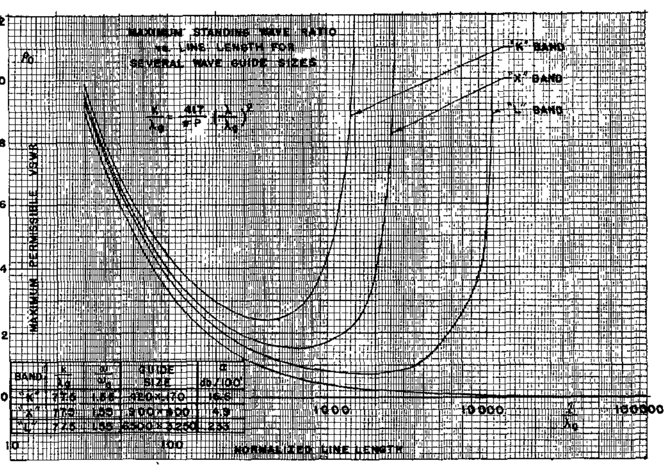

Fig. 6—Maximum standing wave ratio vs line length for several waveguide sizes.

III. Experimental Verification

Experimental verification of the theory developed in Section II was attempted by setting up a 2J42 magnetron (X Band), 10 or 40 feet of $1 \times \frac{1}{2}$ inch waveguide, and a mismatched load adjustable in magnitude and phase. The pulling figure is measured first by observing the total change in frequency when a load with a vswr of 1.5 is varied through all possible phases. This value of P is then used to compute the frequency of oscillation as a function of phase for various vswr's and for 10 feet of waveguide. Figs. 7 and 8 show the results of this computation [from (13)] along with the experimental results. The predicted changes in frequency follow the theoretical changes rather closely for all the values of vswr that were considered. The discrepancies are because of the simplified theory that has been used. A more precise theory, which would take into account the effects of line conductance on magnetron frequency, would probably be more accurate but too unwieldy to be useful practically. The principal purpose of the theory as developed here is to permit predicting unstable conditions and studying remedial measures. For these purposes the experiment shows it to be sufficient. Fig. 8 is the case where the vswr is high enough to cause frequency jumps. For $\rho_l = 2.5$ ($\rho_0 = 2.3$ when the correction for line loss is made) the normalized line conductance has also been plotted. The small numbers represent the phase angle of the load on both the frequency and conductance curves. Note that in the region where there are three possible frequencies of oscillation the magnetron will avoid the frequency where the conductance is high and oscillate at either of the two frequencies where the line conductance is low (cf. Fig. 4). The "high conductance" frequency corresponds to the frequency on Fig. 4 where $d\omega_0/d\omega$ is negative. This condition is not stable in the sense that the magnetron will not stay there with any incremental disturbance.

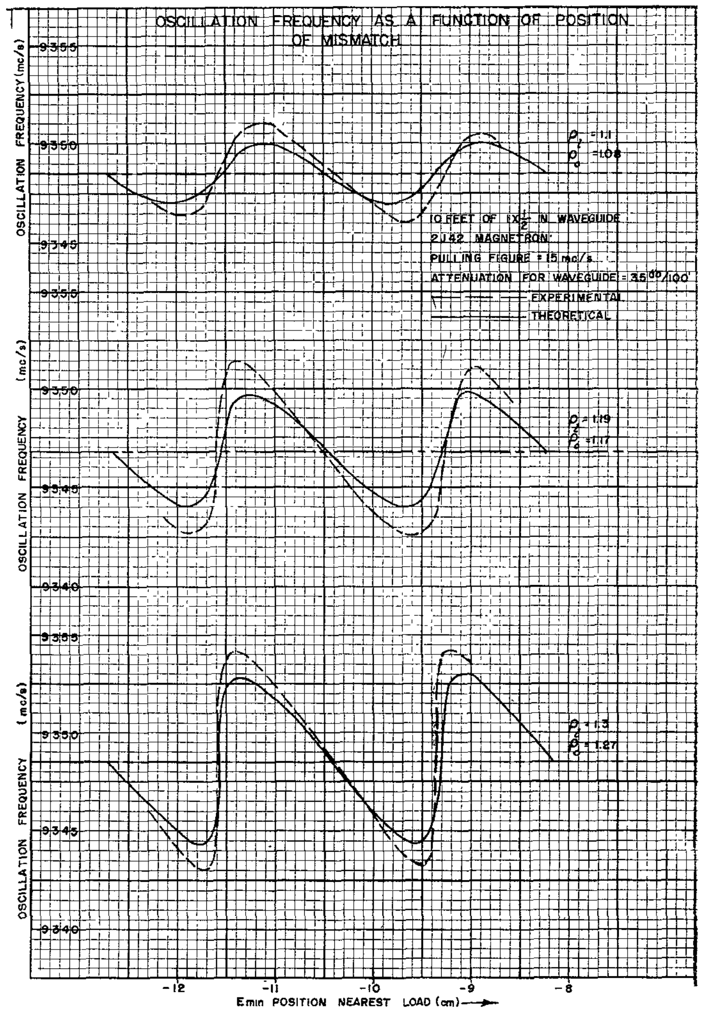

Fig. 7—Oscillation frequency as a function of position of mismatch.

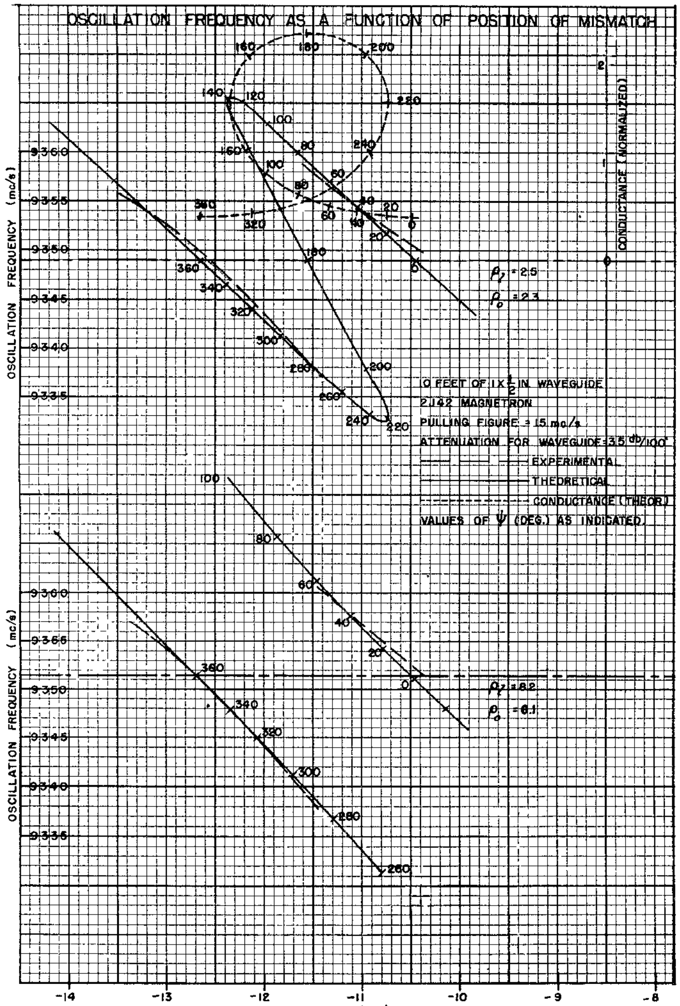

Fig. 8—Oscillation frequency as a function of position of mismatch.

Figs. 9–16 (pp. 38–45) are a series of photographs of rf envelope, spectrum, and instantaneous frequency of a pulsed magnetron under different load conditions. In each case ρ_l, the load vswr, and ρ_0, the vswr corrected for line loss, are shown. When the magnetron is operating stably, the rf spectrum is a single lobe and the instantaneous frequency is single valued. In an unstable condition the spectrum divides into two lobes, and the instantaneous frequency during the pulse becomes distinctly double valued. The two lobes of the spectrum will be separated by approximately the difference between the two principal instantaneous frequencies. Because of "pushing," the instantaneous frequency, even in a stable condition, shows variation during the pulse, but it is still easy to differentiate between incidental frequency modulation and true instability.

For 10 feet of line the critical vswr is 1.27, and reference to Figs. 10 through 13 shows that when ρ_0 is greater than this value, there exists the possibility for frequency jumping if the load phase is appropriate. Fig. 12 shows this clearly. Note also that for a vswr less than critical, but close to it, there is a distinct jitter in the frequency deviation during the pulse and a corresponding broadening of the spectrum. Fig. 14 shows the conditions with a very high vswr and Figs. 15 and 16 the conditions when a very long line (42 feet) is used.

When the load is greater than critical, it is still possible, by varying the phase, to achieve stable operation. Then we have a "quasi-stable" operation. The narrower the pulse (or broader the modulation spectrum) the more difficult it is to achieve quasi-stable operation with a given set of conditions. If the line is long enough, it may be impossible, since the period between skips can become less than the bandwidth needed for modulation.

This series of photographs, besides providing further verification of the theory, shows the deleterious effects of long-line skipping.

Corrective Measures

Long-line effect is best avoided by avoiding the long lines. For example, the transmitter can be located directly after the antenna, or occasionally a 45° mirror can be used instead of a transmission line. This is likely to be difficult if power loss is to be avoided. There still remain, however, many installations where a long transmission line is necessary. In this case, the ideal means to eliminate long-line skipping is a unilateral device which directs the reflected energy into a dummy load instead of returning it to the oscillator.

Several varieties of such devices have been developed using ferrities.[2,3] Most of them fall into two categories: one uses nonreciprocal Faraday rotation to divert the reflected energy into a load and the other uses resonant absorption of the energy returned from the antenna. They have been extremely successful at high frequencies and medium power levels, but materials are still not generally available for use at ultra-high frequencies and for very high average powers.

A brutal solution to the problem is the introduction of attenuation to lower the vswr at the transmitter below the critical value. Obviously, this is not desirable since the over-all efficiency of the system will also be lowered. However, with power to spare, it is often satisfactory. Frequently, a better approach is to decouple the magnetron (or other oscillator) and thus lower its pulling figure. For the usual magnetron coupling values, this will result in less over-all loss in efficiency for a given increase in skip length than will the insertion of loss. Reference to Fig. 2 shows that for high values of P only a very small reduction in η will produce a large reduction in P. In general there exists an optimum compromise between decoupling the oscillator and adding attenuation which will result in the least loss in over-all efficiency for the maximum increase in skip length. This optimum can be computed once the length of line that will be necessary and the best obtainable vswr are known. This calculation is best handled numerically

[2] C. L. Hogan, "The microwave gyrator," *Bell. Sys. Tech. Jour.*, vol. 31, p. 1; January, 1952.

[3] H. Chait and N. Sakiotis, "Properties of ferrites in waveguides," Trans. IRE, vol. MTT-2, pp. 11–16; November, 1953.

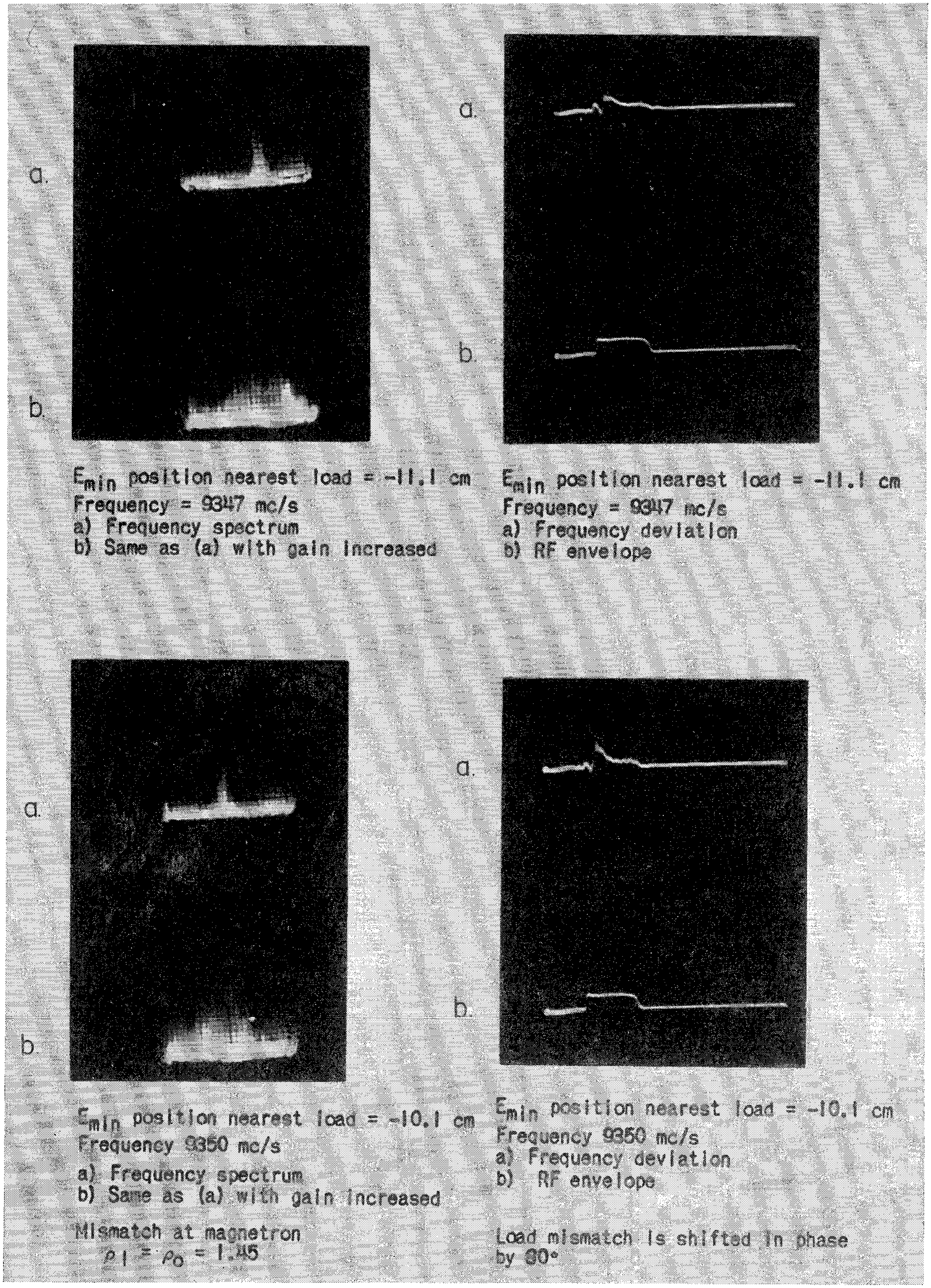

Fig. 9—RF envelope, spectrum, and instantaneous frequency of a pulsed magnetron under different load conditions.

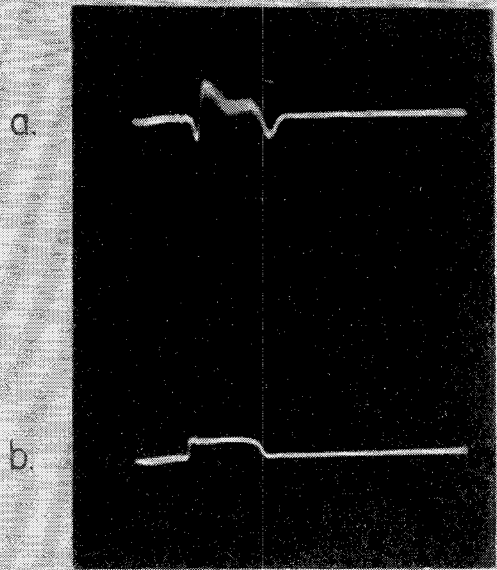

E_{min} position nearest load = -9.05 cm
Frequency = 9350.5 mc/s
a) Frequency deviation
b) RF envelope

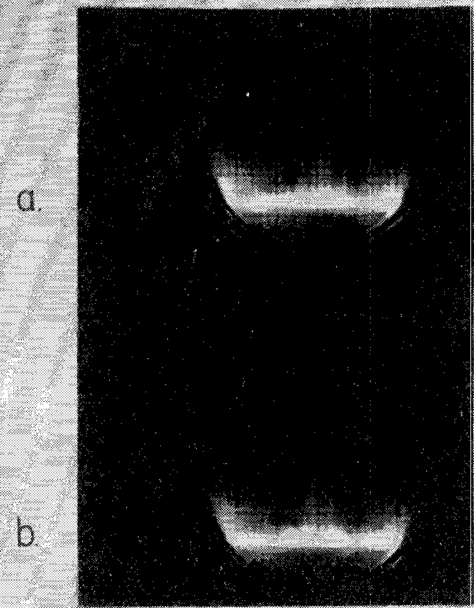

Frequency spectrum
a) E_{min} position nearest load = -9.05 cm
b) E_{min} position nearest load = -10.55 cm

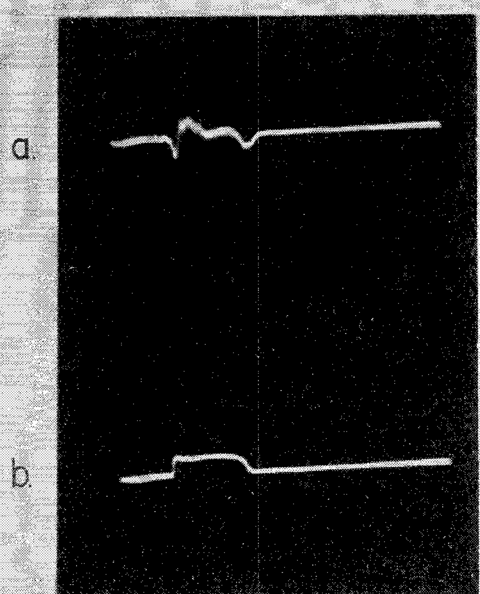

E_{min} position nearest load = -10.55 cm
Frequency = 9349.5 mc/s
a) Frequency deviation
b) RF envelope

10 feet of 1 x 1/2 in. wave guide

$\rho_1 = 1.1$

$\rho_0 = 1.08$

Load mismatch is shifted in phase by 120°

Fig. 10

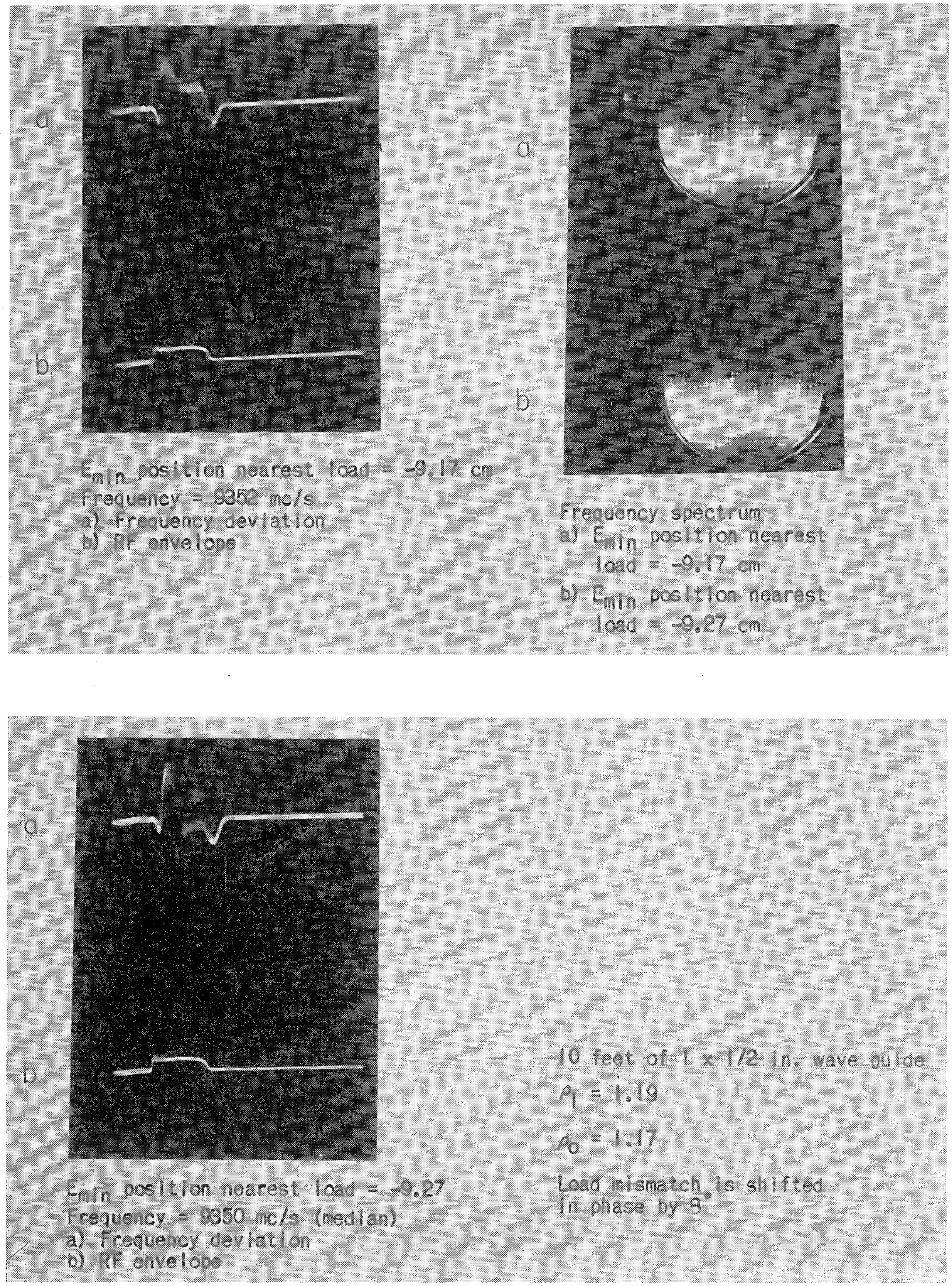
a
b
E_{min} position nearest load = -9.17 cm
Frequency = 9352 mc/s
a) Frequency deviation
b) RF envelope
a
b
Frequency spectrum
a) E_{min} position nearest load = -9.17 cm
b) E_{min} position nearest load = -9.27 cm
a
b
E_{min} position nearest load = -9.27
Frequency = 9350 mc/s (median)
a) Frequency deviation
b) RF envelope
10 feet of 1 x 1/2 in. wave guide
ρ_1 = 1.19
ρ_0 = 1.17
Load mismatch is shifted in phase by 8°

Fig. 11

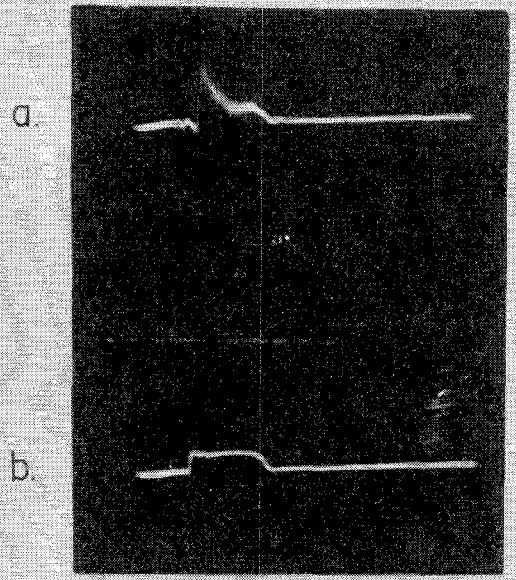

E_{min} position nearest load = -9.52 cm
Frequency = 9343 mc/s
a) Frequency deviation
b) RF envelope

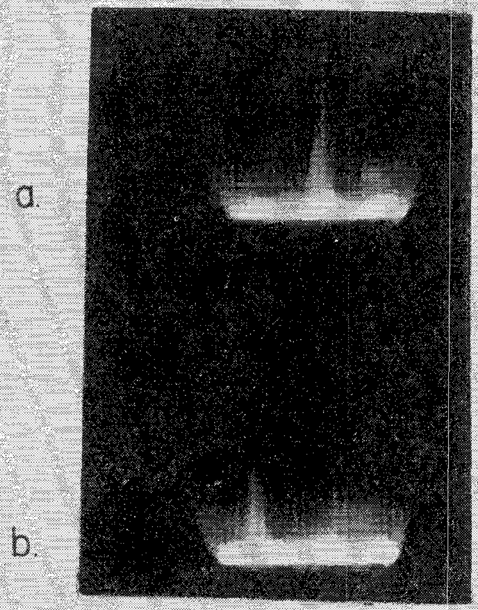

Frequency spectrum
a) E_{min} position nearest load = -9.52 cm
b) E_{min} position nearest load = -9.41 cm
oscillation at two frequencies

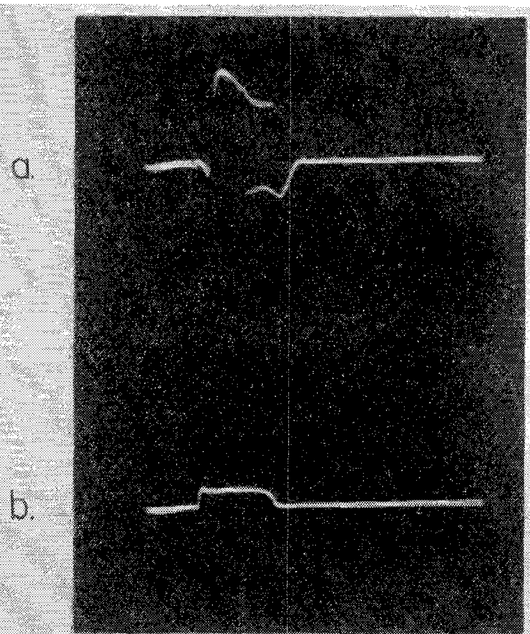

E_{min} position nearest load =-9.41 cm
Frequency = 9343 mc/s and 9353 mc/s
a) Frequency deviation
b) RF envelope

10 feet of 1 x 1/2 in. wave guide

$\rho_1 = 1.3$

$\rho_0 = 1.27$

Load mismatch is shifted in phase by 8.8°

Fig. 12

a.

b.

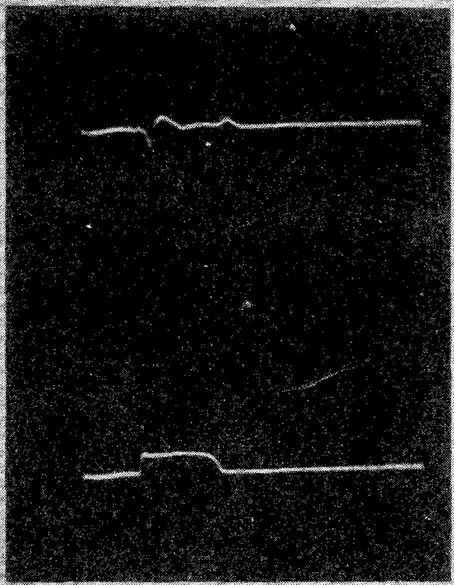

E_{min} position nearest load = -12.83 cm
Frequency = 9351 mc/s
a) Frequency deviation
b) RF envelope

a.

b.

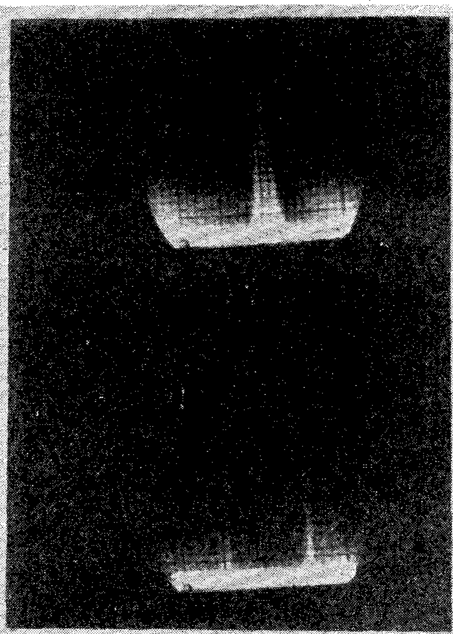

Frequency spectrum
a) E_{min} position nearest load = -12.83 cm
b) E_{min} position nearest load = -11.64 cm

a.

b.

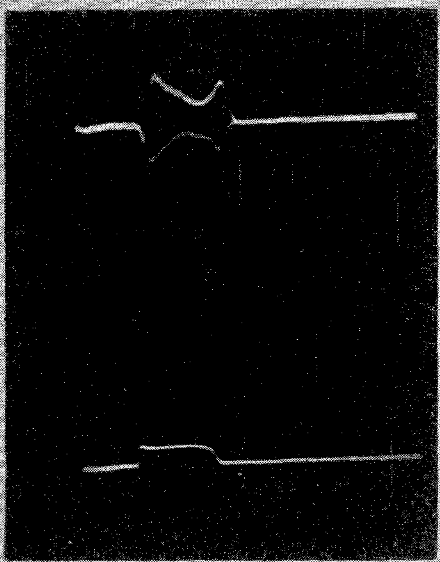

E_{min} position nearest load = -11.64 cm
Frequency = 9339 mc/s and 9360 mc/s
a) Frequency deviation
b) RF envelope

10 feet of 1 x 1/2 in. wave guide

$\rho_1 = 2.5$

$\rho_0 = 2.3$

Load mismatch is shifted in phase by 95.1°

Fig. 13

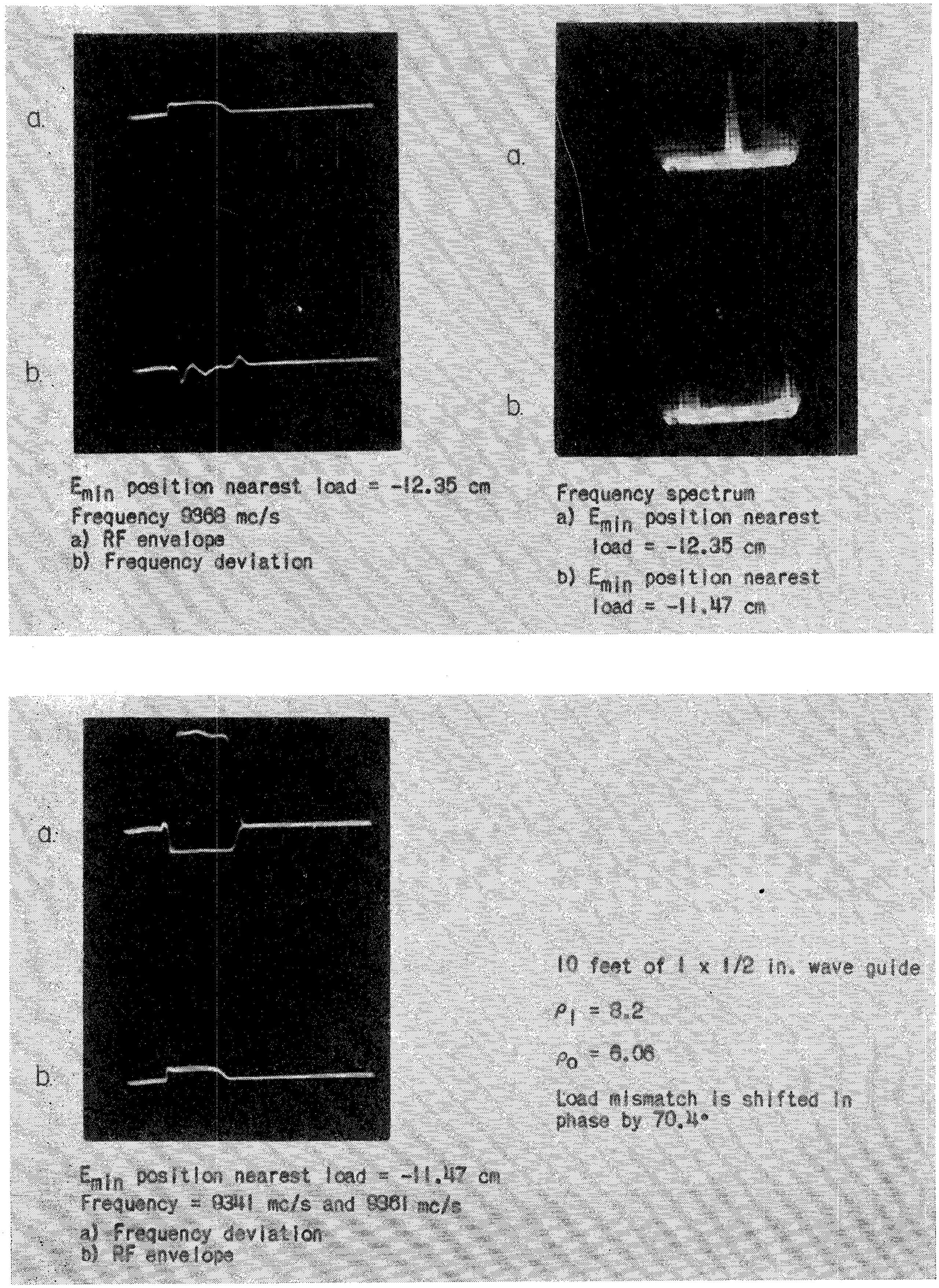
a.
b.
E_{min} position nearest load = -12.35 cm
Frequency 9368 mc/s
a) RF envelope
b) Frequency deviation
a.
b.
Frequency spectrum
a) E_{min} position nearest load = -12.35 cm
b) E_{min} position nearest load = -11.47 cm
a.
b.
E_{min} position nearest load = -11.47 cm
Frequency = 9341 mc/s and 9361 mc/s
a) Frequency deviation
b) RF envelope
10 feet of 1 x 1/2 in. wave guide
ρ_1 = 8.2
ρ_0 = 6.06
Load mismatch is shifted in phase by 70.4°

Fig. 14

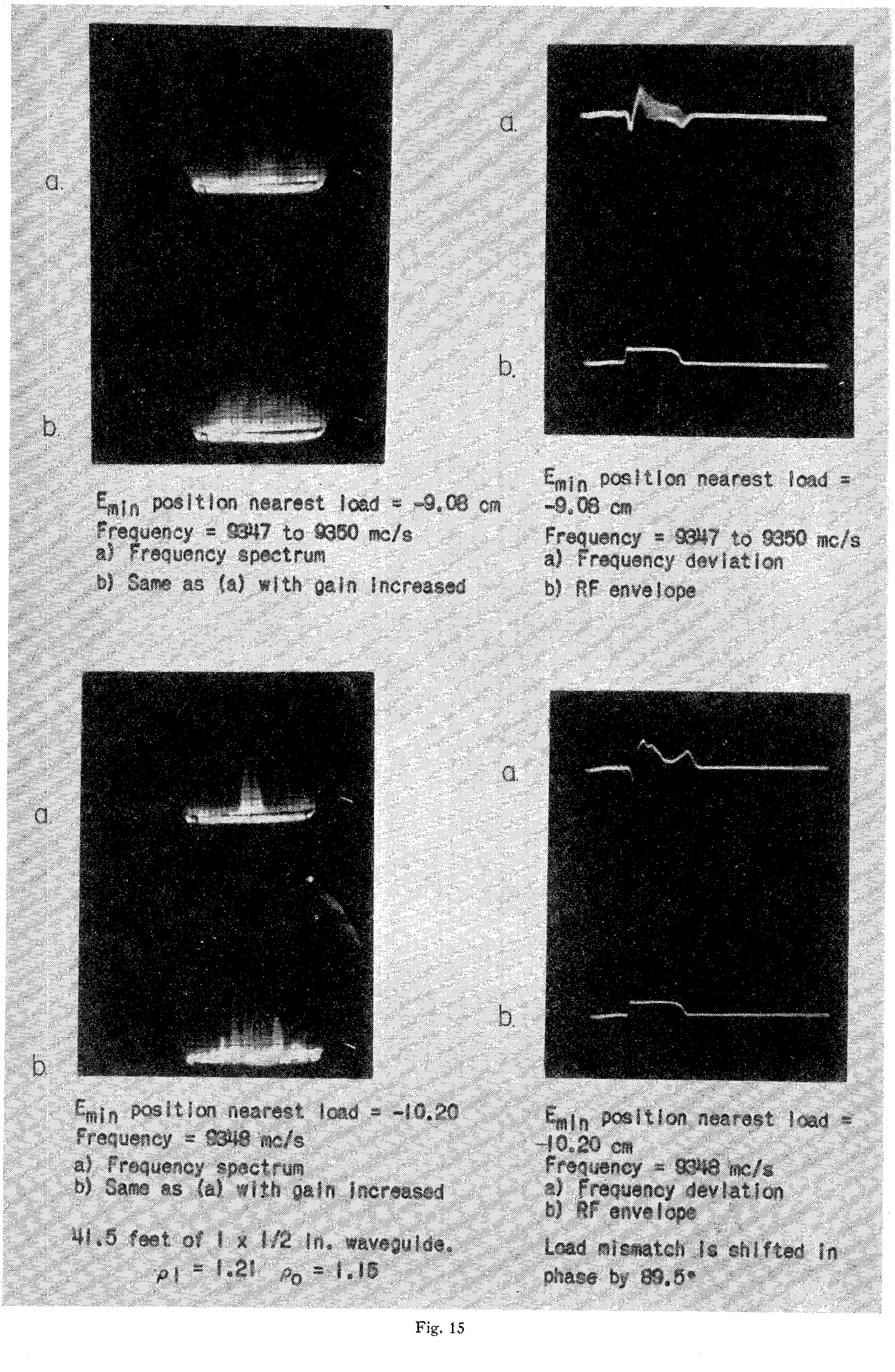
a.
b.
Emin position nearest load = -9.08 cm
Frequency = 9347 to 9350 mc/s
a) Frequency spectrum
b) Same as (a) with gain increased
a.
b.
Emin position nearest load = -9.08 cm
Frequency = 9347 to 9350 mc/s
a) Frequency deviation
b) RF envelope
a.
b.
Emin position nearest load = -10.20
Frequency = 9348 mc/s
a) Frequency spectrum
b) Same as (a) with gain increased
41.5 feet of 1 x 1/2 in. waveguide.
ρl = 1.21 ρo = 1.15
a.
b.
Emin position nearest load = -10.20 cm
Frequency = 9348 mc/s
a) Frequency deviation
b) RF envelope
Load mismatch is shifted in phase by 89.5°

Fig. 15

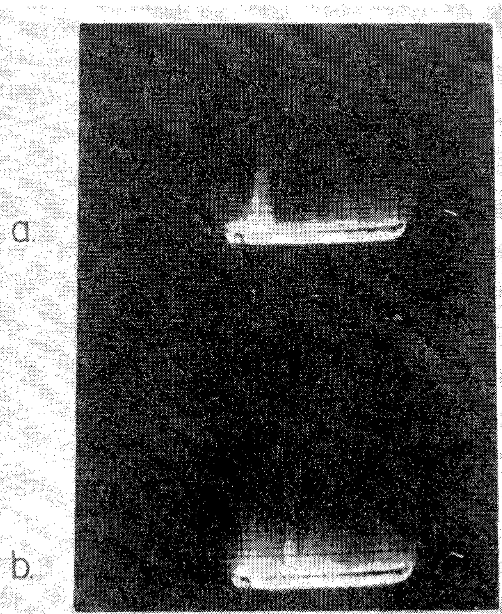

E_{min} position nearest load = -9.28 cm
Frequency = 9348 mc/s and 9353 mc/s
a) Frequency spectrum
b) Same as (a) with gain increased

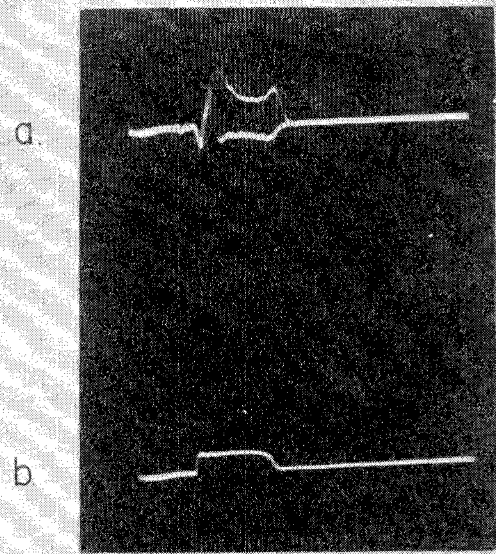

E_{min} position nearest load = -9.28 cm
Frequency = 9348 mc/s and 9353 mc/s
a) Frequency deviation
b) RF envelope

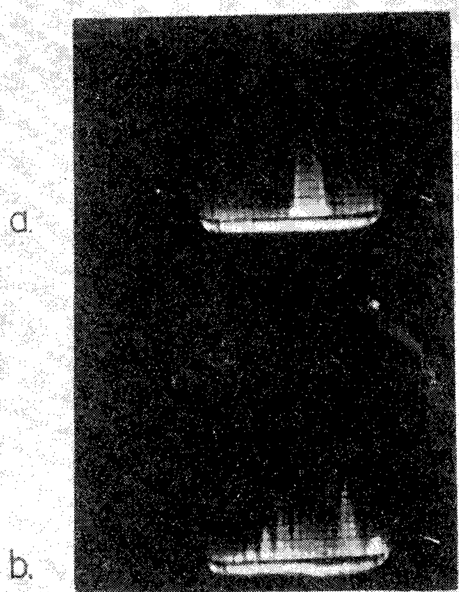

E_{min} position nearest load = -10.4 cm
Frequency = 9348 mc/s
a) Frequency spectrum
b) Same as (a) with gain increased

41.5 feet of 1 x 1/2 in. waveguide
ρ_1 = 1.45 ρ_0 = 1.30

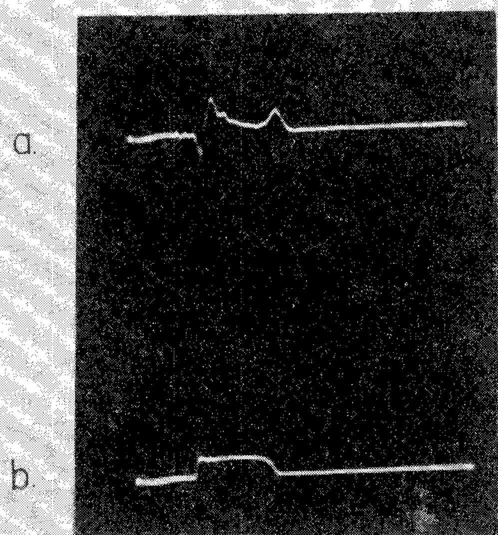

E_{min} position nearest load = -10.4 cm
a) Frequency deviation
b) RF envelope

Load mismatch is shifted in phase by 89.5°

Fig. 16

by using (17) and (18). For a series of assumed values of P the permissible vswr, ρ, is calculated from (17) using a fixed value for l_c. Eq. (9) is then used to compute the magnetron efficiency. If ρ is higher than that which can be obtained with the given load, then (18) is used to compute the attenuation necessary to reduce the load vswr to the permissible value ρ_0. The over-all efficiency is then calculated from the magnetron efficiency and other loss values. The results, plotted vs P, are shown in Fig. 17. Note the maximum value of efficiency is rather broad, leaving some freedom in the tube design. Unfortunately many existing magnetrons are heavily overcoupled to increase the output power and reduce the back heating at the cost of making the over-all equipment design much more difficult.

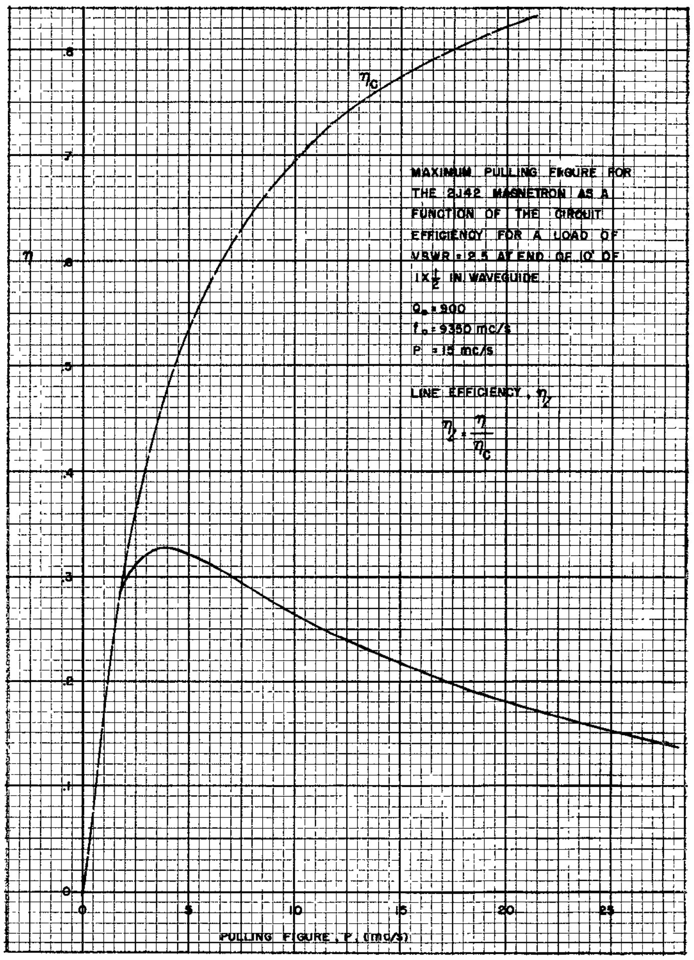

Fig. 17—Maximum pulling figure for the 2J42 magnetron as a function of the circuit efficiency for a load of vswr = 2.5 at end of 10 feet of $1 \times \frac{1}{2}$ inch in waveguide.

If the vswr is not too high, then a phase shifter can be incorporated which will permit quasi-stable operation in between the points of frequency jumping, as discussed in Section III. The wider the modulation bandwidth, the less likely it is that this scheme will be successful. This is particularly true if the line is very long and the frequency separation between "skips" is small.

If magnetron operation is restricted to a narrow band of frequencies and the line length is too long to permit quasi-stable operation, even with a phase shifter, then there is another device which is sometimes successful. A rather large mismatch is introduced in the line considerably closer than the load. The period between skips for this mismatch is greater than the period between skips for the load (antenna). By phasing this mismatch, it will be possible to achieve quasi-stable operation at some reduction in output power. Effectively this is decoupling the magnetron by a cavity formed with a resonant line length. It is a useful and practical cure for long line effect when the system is only to be operated over a narrow frequency range.

List of Symbols

A	Total attenuation of line of length, l.
B	Input susceptance of transmission line.
B_m	Susceptance of magnetron equivalent circuit.
c	Velocity of light in appropriate dielectric.
C	Shunt capacitance of magnetron equivalent circuit.
f	Frequency.
f_1	Maximum oscillation frequency as B is varied.
f_2	Minimum oscillation frequency as B is varied.
G	Shunt conductance of magnetron equivalent circuit.
k	Parameter relating f, P, λ, and λ_g.
l	Length of transmission line.
l_c	Skip length.
n	Transformer turns ratio.
P	Pulling figure.
Q_E	"External Q" of the magnetron.
Q_0	"Unloaded Q" of the magnetron.
Y	Normalized input admittance of a lossless line.
Y_l	Normalized load admittance.
α	Line attenuation per unit length.
β	Coupling factor for magnetron.
Γ	Reflection coefficient of Y_l.
Γ_l	Reflection coefficient at end of transmission line of length, l.
Γ_0	Reflection coefficient at input to transmission line.
η	Over-all efficiency of power transmission to load.
η_c	Coupling efficiency of magnetron.
θ	Electrical length to resistive mismatch.
λ	Wavelength of plane wave in appropriate dielectric.
λ_g	Wavelength in waveguide in appropriate dielectric.
ρ	vswr of load.
ρ_l	vswr at end of transmission line of length, l.
ρ_0	vswr at input to transmission line.
ϕ	Phase of reflection coefficient, Γ.
ψ	$\phi - 2\theta$, phase of Y.
ω	Angular frequency of oscillation.
ω_0	"Natural" resonant frequency of magnetron.
$\Delta\omega$	Change in ω between alternate positions where $\omega = \omega_0$.

Acknowledgment

The author wishes to thank Mr. Setsuo Dairiki of Raytheon Manufacturing Company for the experimental work and photographs.